Supplemental Figure 1

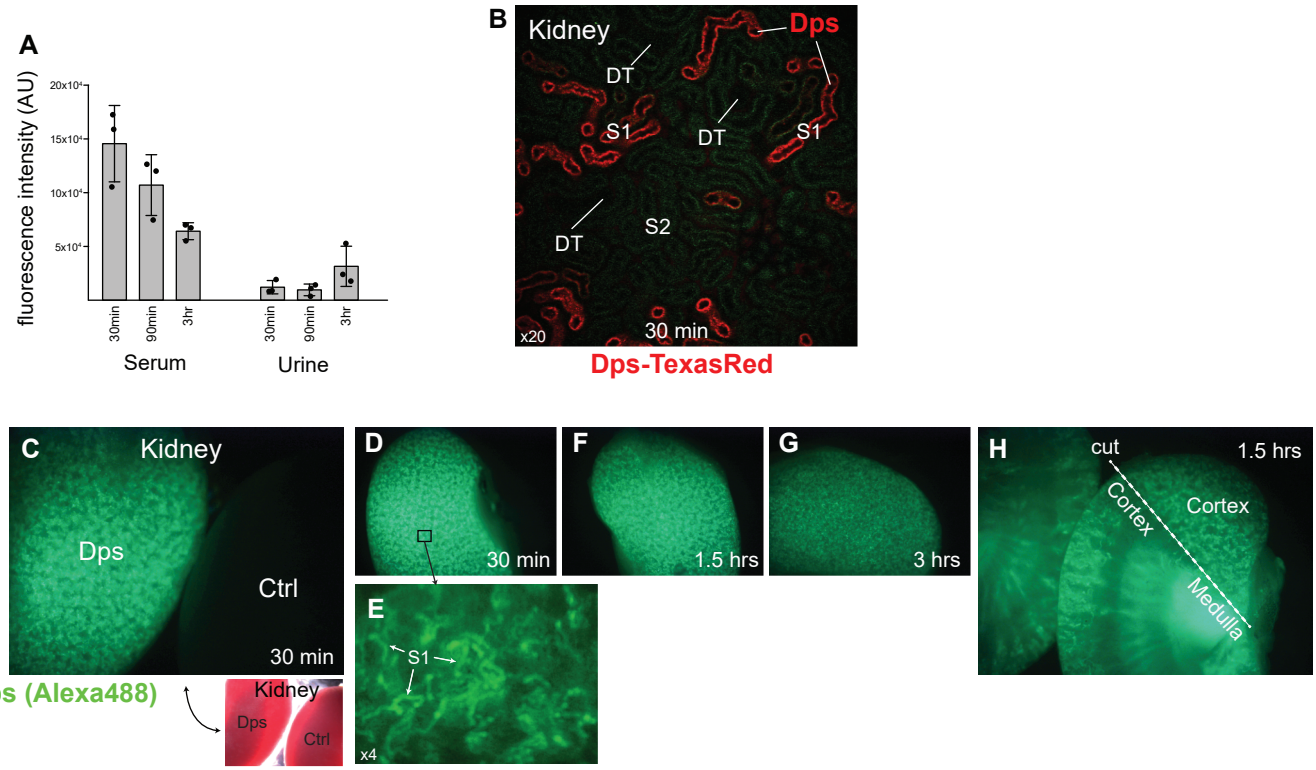

Supplemental Figure 1
(**A**) Quantitation of serum and urine Dps fluorescence intensity for the indicated time points following tail vein injection of Alexa488-Dps (n=3 per time point). (**B**) Low magnification view of Dps distribution in vivo (x20; renal cortex). Note the negligible level of Dps signal in distal tubules/collecting ducts (DT). (**C**) Ex vivo whole kidney imaging 30 min after tail vein injection of Alexa488-Dps. For comparison, a control mouse kidney (PBS vehicle) is shown on the right (inset, bright field). (**D-H**) Ex vivo whole kidney imaging at the indicated time points after Dps iv (original magnification x10 except Fig 1E where x40 is shown; n=3 per time point). (**I-J**) Microscopic examination of sliced kidney tissues 90 min after Dps-Alexa488 tail vein injection (green). In this experiment, Dps was injected into a transgenic mouse that expresses TdTomato exclusively in the endothelial cells (red; Tie2CreER/TdTomato). The bright signal seen in the inner medulla (Suppl Fig 1H) is primarily due to concentrated Dps in the blood rather than urinary lumen. Arrows point to vascular structures in the inner medulla and arrow heads point to urinary lumens. (**K**) Intravital imaging of kidney 30 minutes after Dps iv via the jugular vein. Distribution of Dps administered via jugular vein was identical to that of tail-vein injected Dps. Green 70 kDa dextran was used to highlight blood and interstitial space.

Supplemental Figure 2

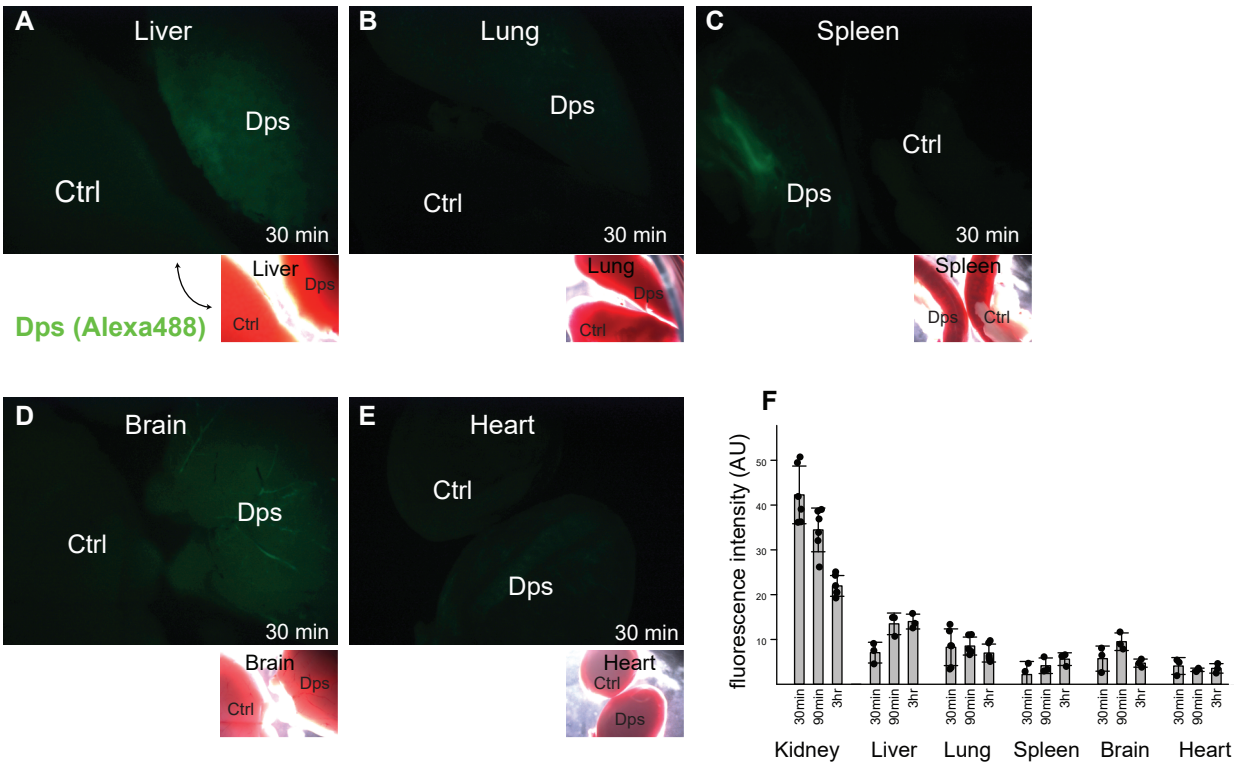

Supplemental Figure 2
(**A-E**) Ex vivo whole organ imaging 30 minutes after intravenous injection of Alexa488-Dps (tail vein). As a reference, control tissues (PBS vehicle) are shown next to corresponding Dps-treated tissues. Original magnification x10. (**F**) Quantitative comparison of Dps distribution for the indicated tissues and time points. Kidney images are shown in Supplemental Figure 1, C-H. n=3 animals per time point (a total of 6 measurements per time point for kidneys and lungs).

Supplemental Figure 3

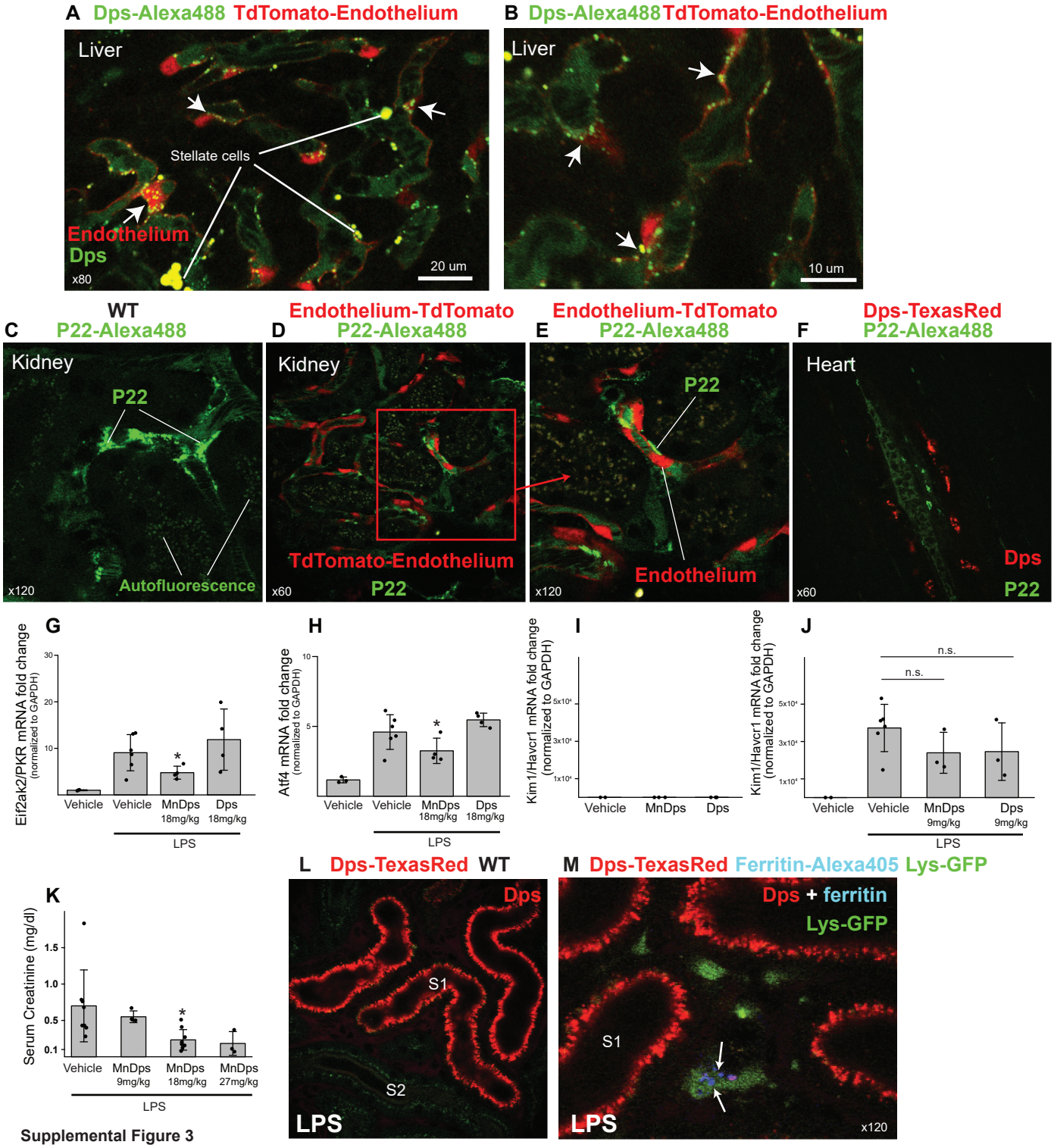

Supplemental Figure 3

(**A-B**) Intravital imaging of the liver 30 min after Dps-Alexa488 tail vein injection (green). Dps was injected into Tie2CreER/TdTomato mice (red). Arrows point to Dps localized in the endothelial cells. (**C**) Distribution of P22 in the kidney, 30 min after jugular vein injection. P22 localized to cells between the renal tubules. (**D-E**) To determine whether P22 is localized to endothelium or other cell types (e.g., pericyte and macrophage/dendritic cells), P22 was injected intravenously to a Tie2CreER/TdTomato transgenic mouse (red). P22 localized to non-endothelial interstitial cells. (**F**) In this experiment, Dps (red) and P22 nanoparticles were co-administered and the freshly isolated heart was imaged ex vivo. No Dps was observed except some around the blood vessels. (**G-H**) Quantitative PCR of kidney tissue Eif2ak2/PKR and Atf4 under indicated conditions, 24 hours after 5 mg/kg LPS i.p. *p<0.05 vs. Dps 18 mg/kg. One-way ANOVA followed by pairwise t tests with corrections for multiple testing using the Benjamini and Hochberg procedure. (**I**) Quantitative PCR of kidney tissue Kim1/Havcr1. Administration of unmodified Dps or MnDps without LPS did not increase the levels of Kim1/Havcr1. (**J**) Kidney tissue Kim1/Havcr1 levels 24 hours after 5 mg/kg LPS i.p. with 9 mg/kg MnDps or unmodified Dps iv as determined with quantitative PCR. LPS was administered immediately after Dps, MnDps or vehicle injection. As opposed to 18 mg/kg, no significant renoprotection was observed with the 9 mg/kg dose in either MnDps or unmodified Dps. The data points for LPS + vehicle are from Figure 3B. (**K**) Serum creatinine levels 24 hours after 5 mg/kg LPS i.p. MnDps were administered at indicated doses immediately before LPS ip. The data points for vehicle and 18mg/kg MnDps are from Figure 3A. *p<0.05 vs. MnDps 9 mg/kg. One-way ANOVA followed by pairwise t tests with corrections for multiple testing using the Benjamini and Hochberg procedure. (**L**) Distribution of Dps in the kidney after LPS challenge (24 hours) was comparable to that of control mice. (**M**) Lys-EGFP transgenic mouse that expresses EGFP in myeloid cells (green) was injected with LPS followed 24 hour later by Dps (red) and ferritin (blue). Ferritin signal was not observed in the proximal tubules. Arrows point to ferritin internalized by a myeloid cell.

Supplemental Figure 4

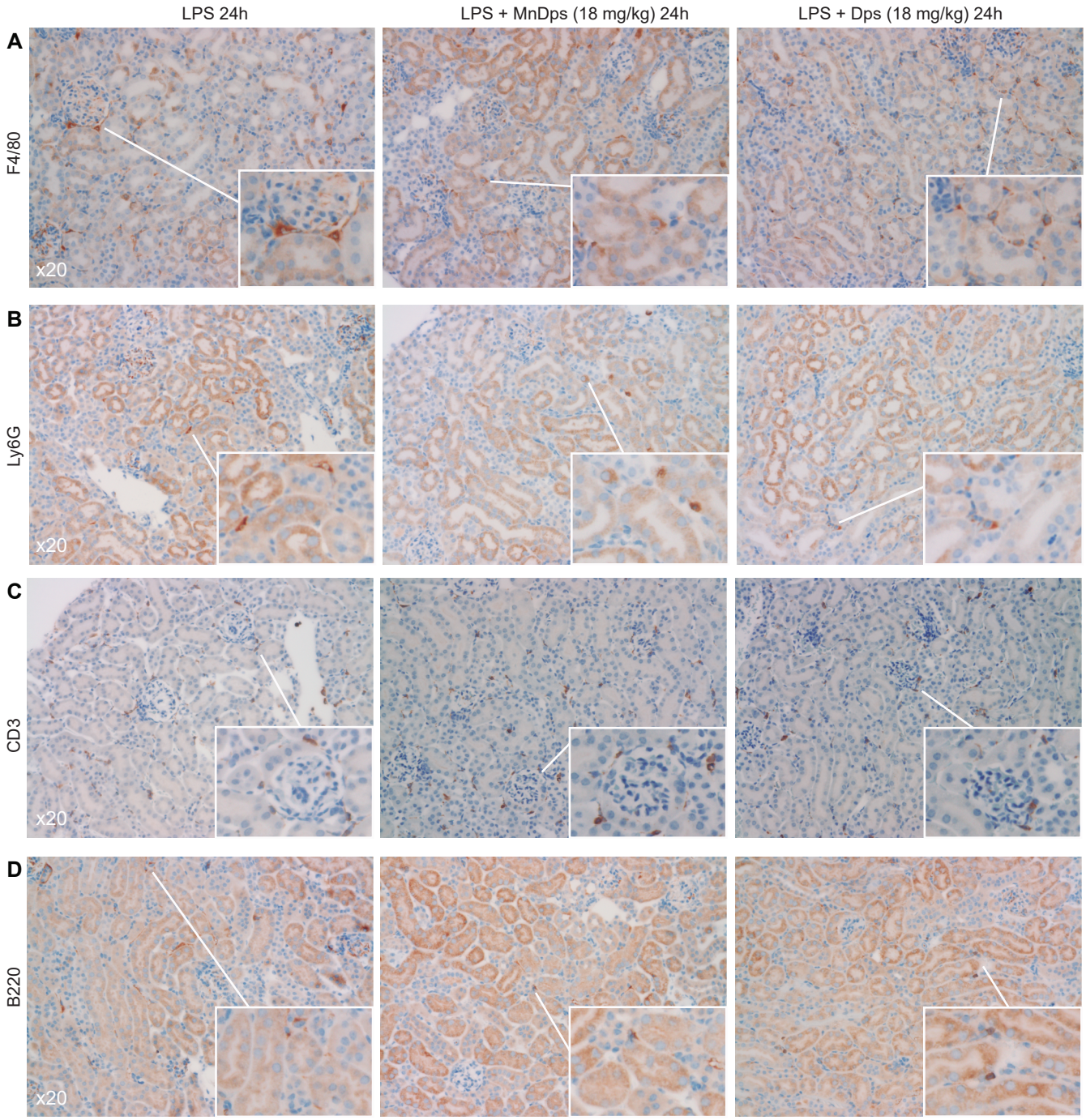

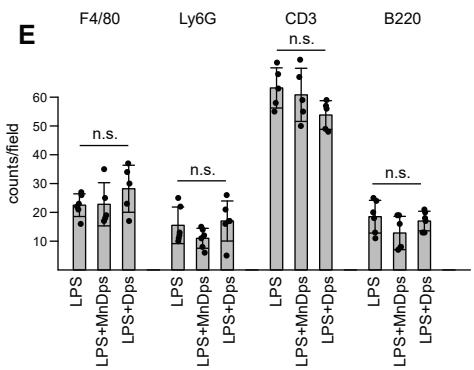

Supplemental Figure 4
(**A-D**) Representative images of F4/80 (macrophages), Ly6G (neutrophils), CD3 (T cells) and B220 (B cells) are shown under indicated conditions. Insets point to magnified views of select areas. (**E**) Quantitation of indicated marker positive cells per field. No statistical significance was found among the conditions by ANOVA.

Supplemental Figure 5

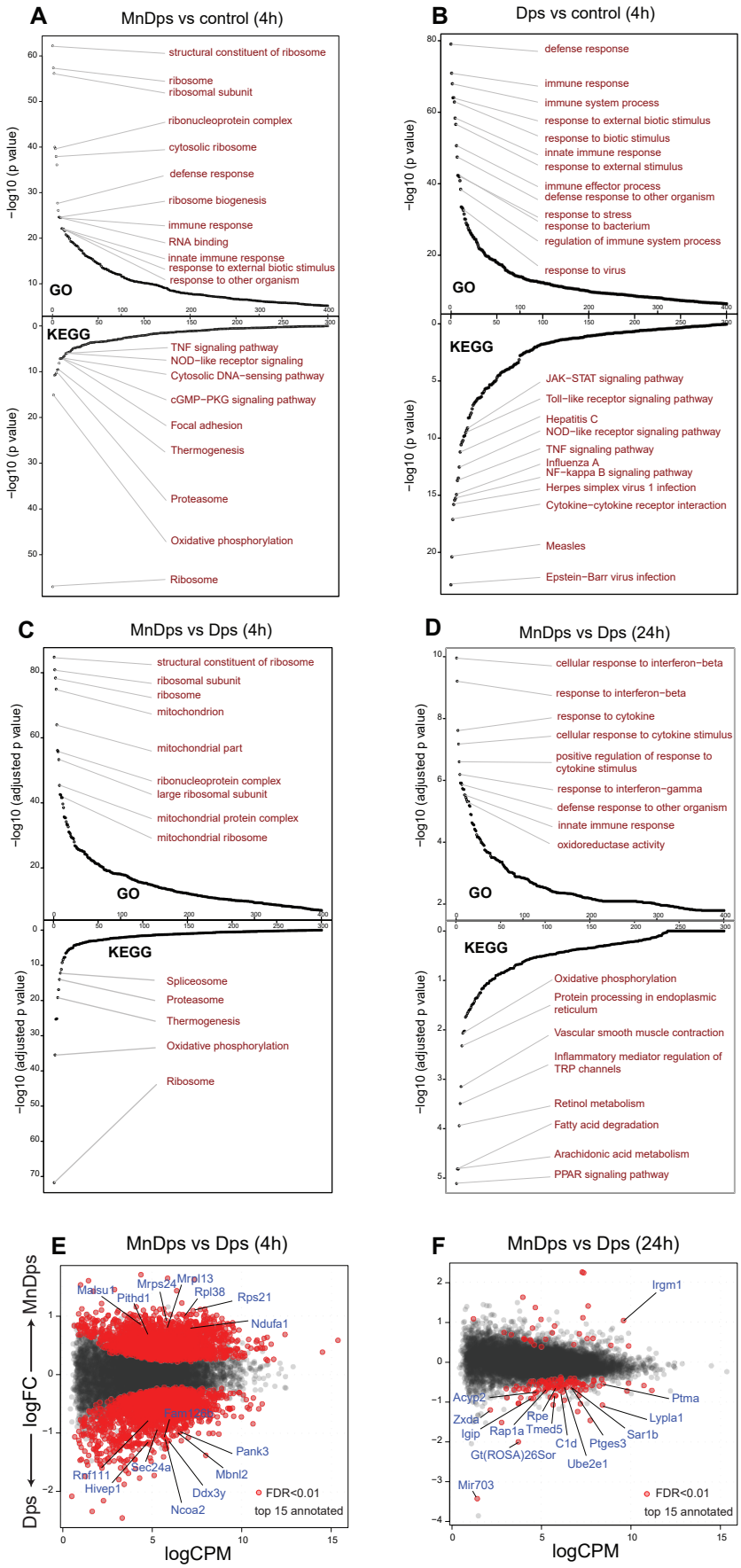

Supplemental Figure 5

(**A**) Pathway enrichment analysis comparing MnDps (4 hours) and vehicle control. Gene Ontology terms (GO) and Kyoto Encyclopedia of Genes and Genomics (KEGG) metabolic pathways are aligned in the order of statistical significance. (**B**) Comparison between Dps (4 hours) and vehicle control. (**C-D**) Pathway enrichment analyses comparing the effects of MnDps versus Dps in kidney tissues at 4 and 24 hours, respectively. (**E-F**) Smear plots for MnDps versus Dps (4 hours and 24 hours) in which differentially expressed genes are highlighted in red. Top 15 differentially expressed genes are annotated in blue.

Supplemental Figure 6

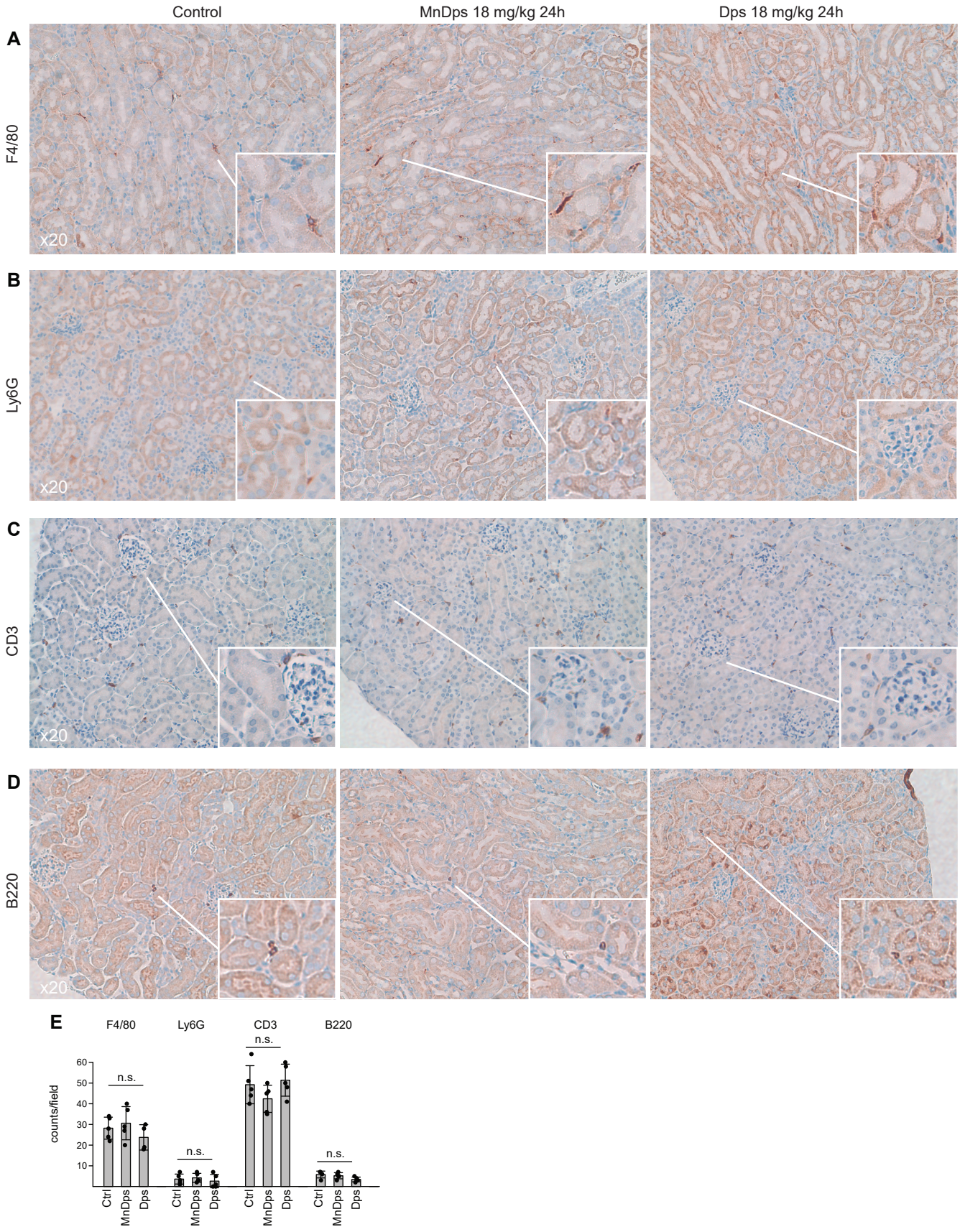

Supplemental Figure 6
(**A-D**) Representative images of F4/80 (macrophages), Ly6G (neutrophils), CD3 (T cells) and B220 (B cells) are shown under indicated conditions. Insets point to magnified views of select areas. (**E**) Quantitation of indicated marker positive cells per field. No statistical significance was found among the conditions by ANOVA.

Supplemental Figure 7

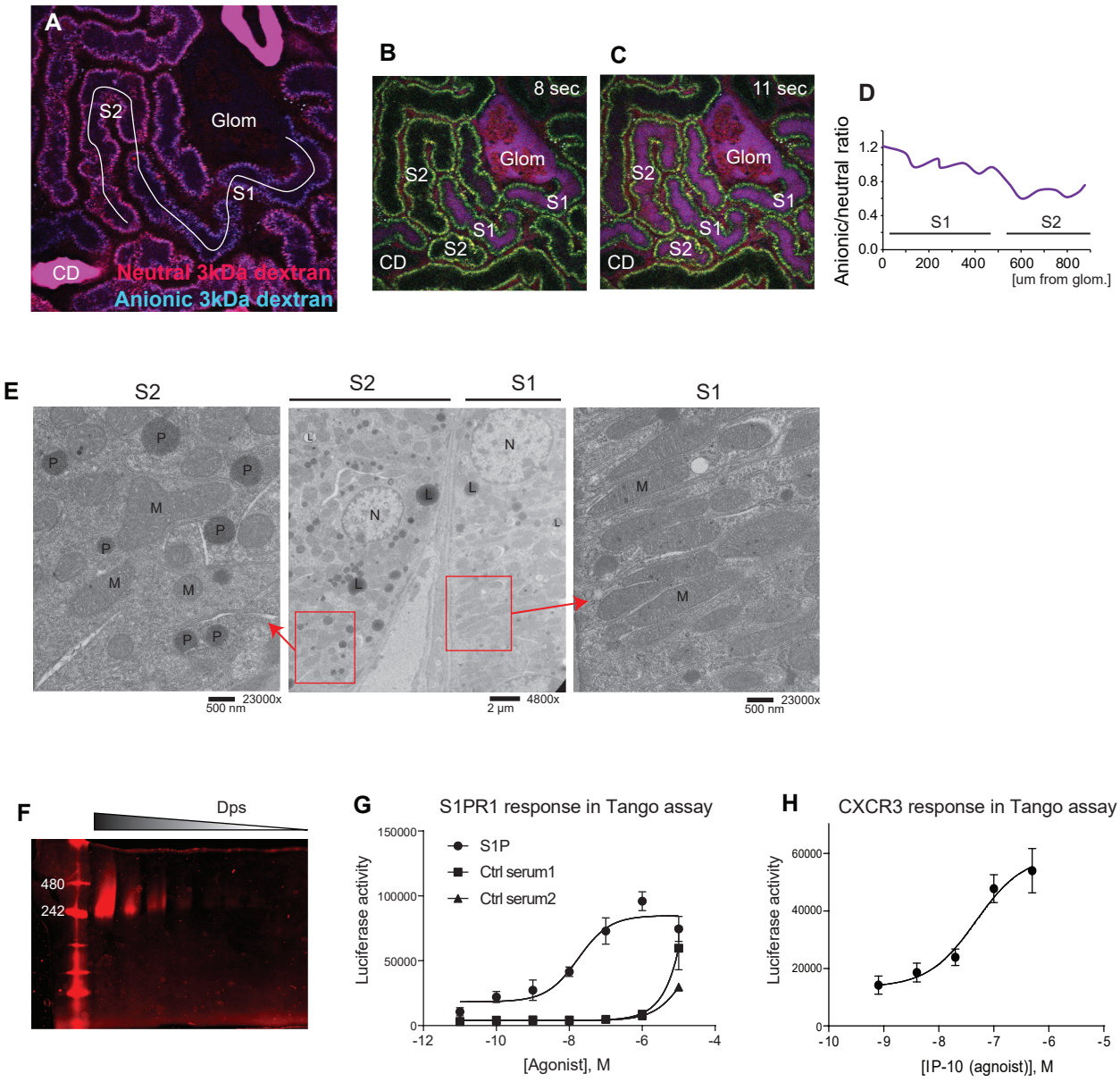

Supplemental Figure 7
(**A-C**) Intravital imaging of the kidney using Munich–Wistar–Frömter rats that have superficial glomeruli accessible to the 2 photon laser. Animals were injected with equal amounts of neutral 3kDa dextran (TexasRed) and anionic 3kDa dextran (CascadeBlue), and the differential uptake of dextrans was determined. Whereas anionic dextran localized to S1 and S2 evenly (blue), neutral dextran preferentially localized to S2 (red). A representative image 20 min after dextran infusion is shown. (**B, C**) S1 and S2 subsegments were determined by the sequential appearance of dextrans in the urinary lumen. (**D**) The ratio of anionic and neutral dextran endocytosis is shown. (**E**) Electron microscopy of S1 and S2 proximal tubules. Peroxisomes are stained black using the alkaline DAB method (51). Note the abundance of peroxisomes in S2 but not in S1. P, peroxisomes; M, mitochondria; N, nucleus; L, lysosomes. (**F**) To confirm the stability of Dps in vitro, native gel western blot analysis was performed 6 weeks after leaving Dps in DPBS buffer with protein cage concentration at 1.5 mg/mL. (**G, H**) Examples of PRESTO-Tango system validation are shown. Using PEI, HTLA cells (30,000 cells/well of 96 well plate) were transfected with S1PR1-Tango vector along with pCX-GFP for transfection efficiency evaluation. S1PR1 agonist S1P or control serum was titrated and incubated overnight (**G**). Similarly, CXCR3 agonist IP-10 was titrated and incubated overnight (**H**).